Experimental study on the liquidus of ladle slags

Jimmy Gran[a] and Du Sichen[b]

a) Swerea MEFOS AB, SE-971 25 Luleå, Sweden

b) Department of Materials Science and Engineering, Royal Institute of Technology, SE-100 44 Stockholm, Sweden.

Abstract: The scope of this work was to experimentally determine the liquidus surfaces in the high basicity region of the Al_2O_3-CaO-MgO-SiO_2 system having moderate Al_2O_3 and SiO_2 contents at steelmaking temperatures. This system is of particular importance for secondary steelmaking slags, not only when considering refining operations, but also for preventive actions to avoid severe refractory corrosion. The existing phase diagram information in the literature is based on a comprehensive experimental study, mainly focusing on blast-furnace slags. These phase diagrams are used extensively by researchers in both steel industry and universities. However the estimated positions of the liquidus lines in the CaO-rich corner are based on very limited experimental data.

In this work, the "equilibrating and quench technique" was employed to find different 2- and 3-phase equilibriums in the CaO rich corner of the Al_2O_3-CaO-MgO-SiO_2 system at 1773 and 1873 K. The Al_2O_3 content was between 25 and 35 mass percent. The samples and the individual phases were quantitatively analyzed by means of EPMA (Electron Probe Micro Analysis) to obtain accurate quantitative data. Based on the EPMA data, phase diagrams were constructed at the 25, 30 and 35 mass % constant alumina planes in the Al_2O_3-CaO-MgO-SiO_2 tetrahedron at silica contents < 20 mass percent. The results generally agreed well with phase diagrams available in the literature with some few exceptions. In addition, the activities of MgO, CaO and Al_2O_3 were estimated, based on solid solution information from the EPMA analysis of solid CaO and MgO.

Keywords: Slag, Al_2O_3-CaO-MgO-SiO_2, secondary steelmaking, EPMA analysis, activity.

1. Introduction

In most operations in secondary steelmaking, a synthetic slag based on the Al_2O_3-CaO-MgO-SiO_2 system is added for refining. In order to get good kinetic conditions for different refining operations, the steel producers very often prefer a completely liquid slag. At the same time, slags that are far from saturated with respect to the refractory oxide will cause severe refractory consumption. Recommended phase diagrams for the Al_2O_3-CaO-MgO-SiO_2 system can be found in Slag Atlas [1], which is based on a number of studies. Most of the work was done by Osborn et al. [2] with some modifications by Gutt and Russel [3] as well as Cavalier and Sandrea-Deudon [4]. However, as stated by Osborn et al. [2], the accuracy of the position of the liquidus line in the basic slag region might be low in the Al_2O_3-CaO-MgO-SiO_2 system in comparison with the area for blast furnace slags. These lines are indicated with a dashed line in their presentation. The work by Cavalier and Sandrea-Deudon [4] is basically a re-calculation using the result from Osborn et al. [2] and the four ternary systems

with some additional experiments in the high silica (25-45 mass%) region. In the work by Gutt and Russel [3], the scope of the investigations was slags with higher SiO_2 contents, with no additional information in the CaO-rich part of the system at steelmaking temperatures. Some disagreements between experimental results and the diagram from Osborn et al. [2] were found by Dahl et al. [5].

In the present work, the liquidus surfaces in the high basicity region of the Al_2O_3-CaO-MgO-SiO_2 quaternary are determined experimentally using the quench technique. The primary interest is the liquidus surfaces of MgO and CaO as primary phases for alumina contents between 25 and 35 mass percent. A thorough survey is needed as there is discrepancy between some results from a recent work [5] and the well-established work by Osborn et al.[2]. This study will help decision-making of slag praxis in steelworks, both with respect to having a completely liquid slag and to reduce refractory consumption. The activities of CaO, MgO and Al_2O_3 are also discussed based on the phase diagram information.

2. Experimental

Oxide powders of Al_2O_3 (99.997%), CaO (99.95%), MgO (99.95%) and SiO_2 (99.8%), all supplied by Alfa Aesar, were calcinated at 1373K to remove moisture and CO_2. After mixing in an agate mortar, about 0.5 g of the powder was put in a Pt-crucible. The sample(s) together with a B-type thermocouple were placed in the even temperature zone of the furnace, with special attention to placing the thermocouple as close to the sample as possible (less than 5 mm). The experimental setup is schematically shown in **figure 1**. The furnace used was a vertical tube furnace with alumina as working tube and $MoSi_2$ heating elements. The furnace was first heated to 30 K above the equilibrium temperature to homogenize the sample. Thereafter the temperature was slowly decreased to 50 K below the equilibration temperature to promote crystallization of solid phases. After heating to the equilibration temperature, the sample was held there for 36 hours before it was dropped into cold water. After quenching, the samples were directly washed with ethanol to prevent hydration. The samples were mounted in conductive embedding material and polished with ethanol as coolant for SEM-EDS analysis. A preliminary SEM-EDS analysis was performed with a Hitachi S-3700N in order to determine the phases present. In the next step, on the basis of the first SEM-EDS analysis, a quantitative EPMA (Electron Probe Microanalysis) was done to determine the composition of the individual phases. Six points in the liquid phase and, if possible, six particles of each solid phase were analyzed with EPMA. The fallowing conditions were used for the EPMA analysis; an accelerating potential of 15kV, a beam current of 50 nA and a probe diameter of 1 μm. For the analysis of Ca and Si, $CaSiO_3$ was used as standard. The analyzing crystal used was Pentaerythritol (PETJ, J: designated for high reflectivity crystal). For the analysis of Al and Mg, the analyzing crystal used was thallium acid phthalate (TAP). Al_2O_3 and MgO were used as standards respectively. The composition of CaO SiO_2, Al_2O_3 and MgO were calculated using ZAF correction method.

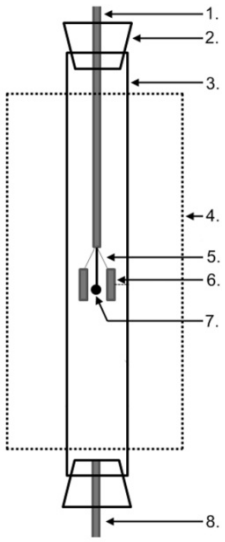

Figure 1. The experimental setup used in the phase diagram study, 1. gas outlet; 2. Silicone rubber stopper; 3. alumina reaction tube; 4. Furnace shell; 5. Pt-wire holding the crucibles; 6. Pt-crucibles containing the samples; 7. B-type thermocouple; 8. Gas inlet.

3. Results

An example of a typical SEM microphotograph can be seen for sample 46 in **figure 2**. Three phases coexist in this sample; liquid, MgO and CaO. The dark phase is MgO, the light grey phase is CaO and the grey matrix is the super cooled liquid. The black area in the lower part of the image is embedding material. The results of the EPMA analysis of the liquid phase together with the solid phases found along with the experimental temperature for each sample can be seen in **table 1**.

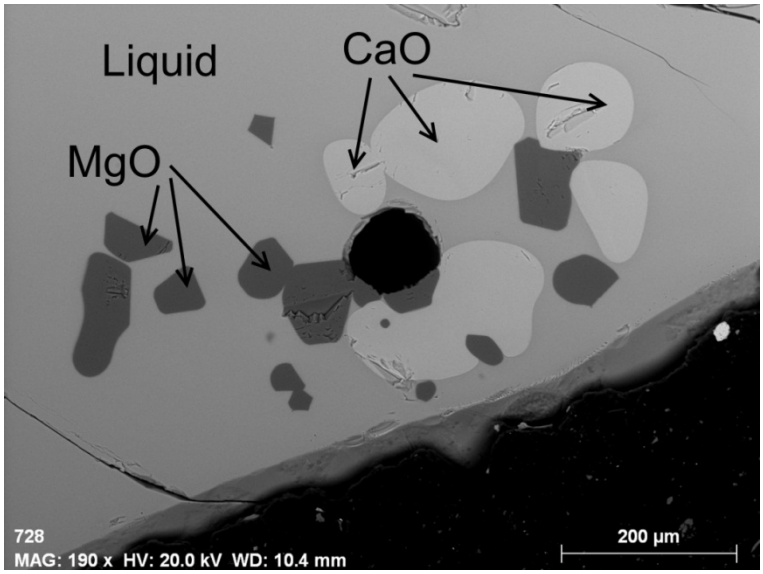

Figure 2. SEM microphotograph showing the coexistence of liquid, MgO and CaO (sample 46). Dark phase: MgO, Light grey phase: CaO, Grey matrix: super cooled liquid.

Table 1. The results of the EPMA analysis of the liquid phase together with the solid phases found along with the experimental temperature for each sample.

Sample No.	T (K)	Phases present	Composition of the liquid phase (mass%)				Sample No.	T (K)	Phases present	Composition of the liquid phase (mass%)			
			CaO	Al_2O_3	SiO_2	MgO				CaO	Al_2O_3	SiO_2	MgO
1	1773	L,M	53.8	30.7	8.5	6.9	51	1873	L,2CS	50.9	27.9	17.6	3.6
2	1773	L,M	48.4	29.6	13.5	8.4	52	1873	L,M	48.6	26.2	14.8	10.4
3	1773	L,M	52.4	31.9	8.5	7.3	53	1873	L,M	52.0	26.0	12.8	9.2
4	1773	L,M	49.8	32.1	10.7	8.0	54	1873	L,2CS	59.5	25.2	13.3	2.0
5	1773	L,M	40.7	30.8	16.9	11.6	55	1873	L,C	59.0	25.8	12.2	3.0
6	1773	L,M,S	38.3	30.5	18.4	12.7	56	1873	L,2CS	56.1	27.7	13.9	2.3
7	1773	L,M	43.8	30.8	15.4	10.0	57	1873	L,2CS	52.9	28.6	15.5	3.0
8	1773	L,M	42.6	30.9	16.1	10.5	58	1873	L,C	57.7	26.8	11.3	4.2
9	1773	L,M	47.3	31.5	12.4	8.7	59	1873	L,C	56.0	26.4	10.5	7.1
10	1773	L, 2CS	48.8	31.0	14.7	5.4	60	1873	L,M	47.5	26.9	15.0	10.5
11	1773	L, 2CS	53.4	30.6	11.8	4.2	61	1873	L,M	51.6	26.8	12.2	9.4
12	1773	L,C	56.0	32.5	8.6	2.9	62	1873	L,2CS	58.4	26.2	13.6	1.8
13	1773	L,C,M	54.6	29.6	8.8	6.9	63	1873	L,C	58.8	26.5	11.8	2.9
14	1773	L,2CS	46.5	30.9	18.0	4.6	64	1873	L	43.8	30.1	15.0	11.1
15	1773	L, 2CS	55.0	31.9	10.3	2.9	65	1873	L	59.0	26.4	12.9	1.6
16	1773	L,C	57.1	32.1	8.4	2.4	66	1773	L,M	51.5	36.3	4.8	7.4
17	1773	L,M	44.7	30.5	14.9	9.9	67	1773	L,M	50.8	34.5	7.1	7.6
18	1773	L,C	59.2	32.0	8.2	0.5	68	1773	L,M	48.6	34.8	8.5	8.1
19	1773	L,C	56.0	31.4	8.2	4.4	69	1773	L,M	43.2	35.3	11.7	9.8
20	1773	L,2CS	57.7	31.0	9.2	2.0	70	1773	L,M	42.6	34.5	12.5	10.3
21	1773	L,C	56.2	31.8	7.8	4.2	71	1773	L,M, MA	37.4	31.0	18.6	13.0
22	1773	L,2CS	57.3	31.4	9.1	2.1	72	1773	L	53.3	34.0	5.5	7.1
23	1873	L,M	52.7	30.1	8.5	8.7	73	1773	L	55.2	33.4	6.5	4.9
24	1873	L,M	45.2	30.0	13.5	11.3	74	1773	L	58.0	35.7	5.8	0.5
25	1873	L,M	51.5	31.2	8.4	8.9	75	1773	L,MA	39.2	32.6	18.9	9.3
26	1873	L,M	47.7	31.5	10.5	10.3	76	1773	L,C	58.7	35.6	5.7	0.0
27	1873	L,M	52.9	31.0	7.0	9.0	77	1773	L,M	52.9	35.0	4.9	7.2
28	1873	L	38.1	31.4	16.2	14.3	78	1773	L,C	57.5	34.4	5.8	2.3
29	1873	L,M	42.1	31.7	13.8	12.3	79	1773	L,C	54.7	34.6	5.9	4.8
30	1873	L	52.1	30.6	8.2	9.1	80	1773	L,C	53.8	34.1	5.8	6.3
31	1873	L,C	60.0	32.0	8.0	0.0	81	1873	L,M	52.4	36.1	2.5	9.0
32	1873	L,C	56.6	30.4	7.5	5.5	82	1873	L,M	49.7	36.1	4.6	9.5
33	1873	L,C	57.0	32.2	6.6	4.2	83	1873	L	46.5	36.7	6.6	10.2
34	1873	L,C	55.1	31.8	6.4	6.7	84	1873	L,M	45.6	36.7	7.1	10.6
35	1873	L,C	61.5	36.7	1.3	0.5	85	1873	L,C	54.3	34.5	3.0	8.3
36	1873	L,C	60.9	35.3	1.3	2.5	86	1873	L,C	56.2	36.9	3.5	3.4
37	1873	L,M	45.5	32.0	11.2	11.2	87	1873	L,M	47.7	37.9	4.4	10.0
38	1873	L,M	35.6	30.4	18.0	16.1	88	1873	L,M	50.8	37.8	2.1	9.3
39	1873	L,C	54.0	31.5	5.9	8.6	89	1873	L,M	39.3	37.3	10.3	13.1
40	1873	L,C	60.3	31.8	7.9	0.0	90	1873	L,M	41.2	36.3	10.3	12.3
41	1873	L,C	59.3	34.0	6.7	0.0	91	1873	L,C	54.9	38.1	1.7	5.3
42	1873	L,C	60.3	32.5	7.1	0.1	92	1873	L	56.5	37.4	3.1	2.9
43	1873	L	33.5	30.1	19.7	16.7	93	1873	L,C	57.4	39.9	1.8	0.9
44	1873	L,M	51.5	25.6	13.5	9.4	94	1873	L,C	54.3	38.4	1.0	6.3
45	1873	L,M	56.0	25.9	9.7	8.4	95	1873	L,C	57.7	38.8	3.5	0.0
46	1873	L,M,C	54.7	27.5	9.0	8.8	96	1873	L	39.3	34.4	12.9	13.4
47	1873	L,C	56.2	26.6	9.5	7.7	97	1873	L	34.6	34.6	15.5	15.3
48	1873	L,M,C	55.0	27.5	9.0	8.5	98	1873	L,M,MA	31.8	33.8	16.7	17.7
49	1873	L,C	58.8	25.1	11.9	4.1	99	1873	L,MA	33.5	32.7	16.9	16.9
50	1873	L,2CS	56.1	27.9	13.6	2.5	100	1873	L,M, C	52.9	35.2	2.9	9.0

4. Discussion

4.1 Presentation of the liquidus lines

In the preparation of the samples, all the compositions have been aimed at in either the 25, 30 or 35 mass% Al_2O_3 section. However, as none of the experimental points lies exactly on these sections, a normalization of the sample composition is necessary for the visual presentation. The normalization is done according to the following procedure: the alumina content is adjusted to 25, 30 or 35 mass %, while the compositions of the rest of the components are normalized in proportion to their original fractions with their sum being either 65, 70 or 75 mass%. As the normalized composition will shift away from the true liquidus surface of the tetrahedron, only the points with a moderate deviation (up to ± 2.5 mass % Al_2O_3) are considered in the graphical presentation. Note that readers should use the data in table 1, if any thermodynamic calculation is carried out.

Figures 3-5 present the experimentally determined liquidus lines in the sections of 25, 30 and 35 mass% Al_2O_3, respectively. In the 25 mass % Al_2O_3 section, lines for 1873 K are presented, while in the 30 and 35 mass % Al_2O_3 section, lines for both 1773 and 1873 K are presented.

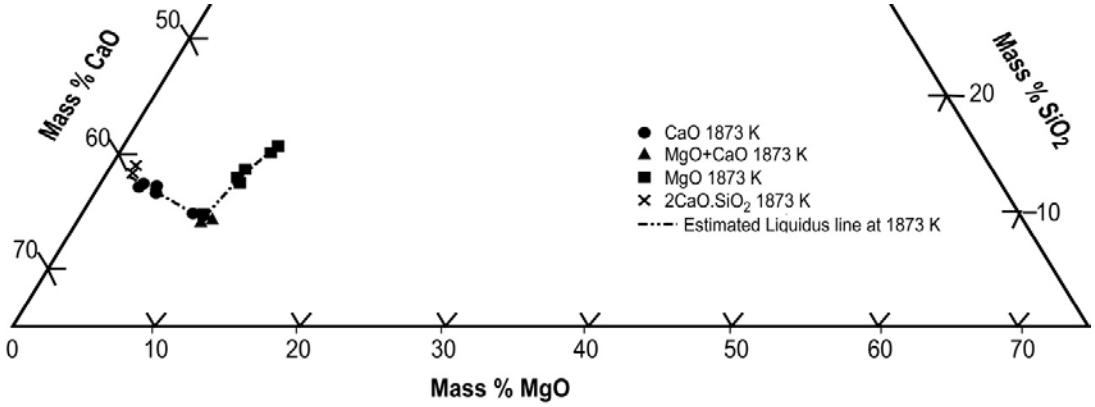

Figure 3. Graphical presentation of the experimental results projected on the section of 25 mass% Al_2O_3 in the quaternary Al_2O_3-CaO-MgO-SiO_2 system.

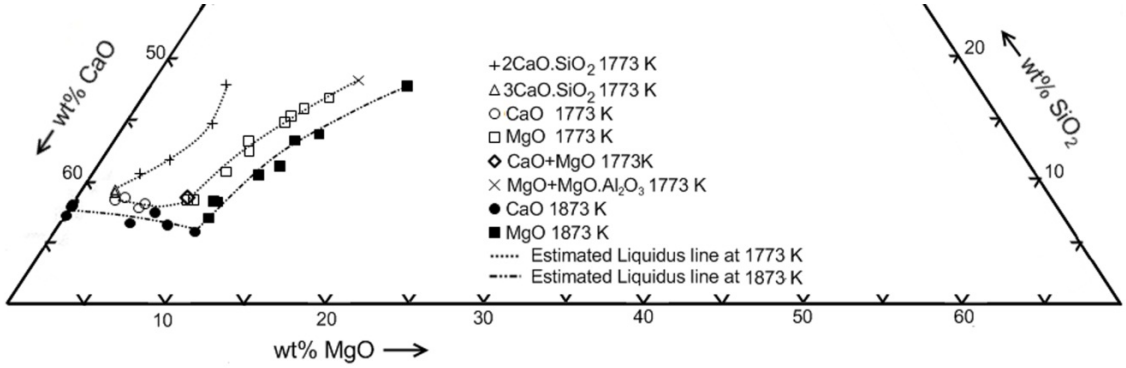

Figure 4. Graphical presentation of the experimental results projected on the section of 30 mass% Al_2O_3 in the quaternary Al_2O_3-CaO-MgO-SiO_2 system.

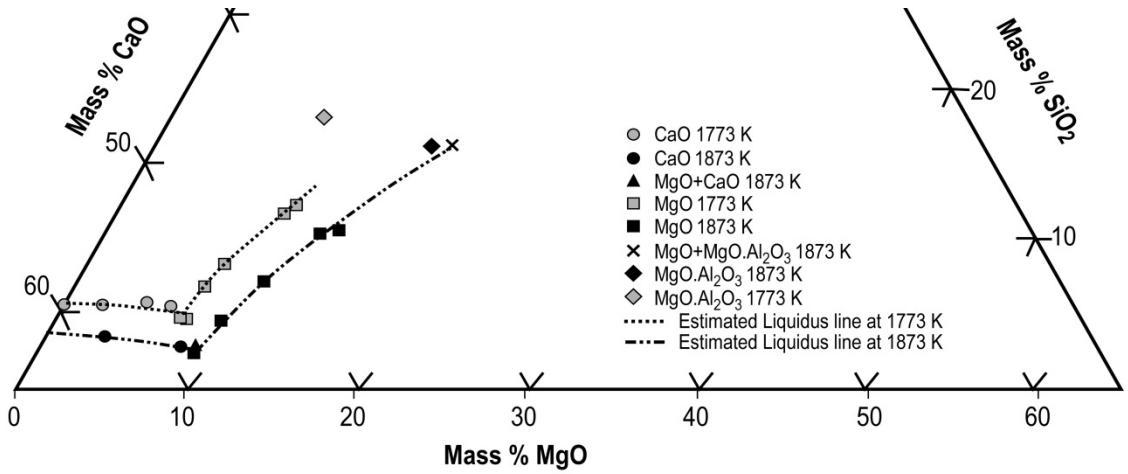

Figure 5. Graphical presentation of the experimental results projected on the section of 35 mass% Al_2O_3 in the quaternary Al_2O_3-CaO-MgO-SiO_2 system

The different phase relationships are marked by different symbols. For example, "●" stands for the liquid in equilibrium with CaO at 1873 K; and "■" stands for the liquid in equilibrium with MgO at 1873 K.

The experimental points are compared with the results from Osborn et al. [2] in **figures 6-8**. For the 25 mass% Al_2O_3 section, the results generally agree well with the lines suggested by Osborn et al. [2]. The present results show a slightly lower solubility of CaO and a higher solubility of MgO. At SiO_2 contents around 17 mass%, the liquidus line for the liquid-MgO equilibrium seems to shift to the right in figure 6, being closer to the 1923 K line suggested by Osborn et al. [2]. The present results show that the liquidus line for CaO saturation is shifted upwards compared to that of Osborn et al [2]. It is also interesting that no $3CaO.SiO_2$ were detected despite the large amount of samples in this area. However, it can't be concluded that this phase does not exist in this section. The several samples related to the liquid-$2CaO.SiO_2$ equilibrium suggest that the solubility of $2CaO.SiO_2$ should be somewhat higher compared to the results of Osborn et al. [2].

For the 30 mass % alumina section, in the case of 1873 K, the experimental compositions of the liquid in equilibrium with CaO agree very well with the solubility line suggested by Osborn et al. [2], while the present experimental results show somewhat higher solubility of MgO. At SiO_2 contents around 10 mass%, the liquid compositions in equilibrium with MgO seem to lie on the line of 1923 K suggested by Osborn et al. [2].

For 30 mass % alumina section, at 1773 K, the experimentally determined solubility lines for both MgO and CaO are in good agreement with the phase diagram suggested by Osborn et al. [2]. On the other hand, the liquidus isotherm for $2CaO.SiO_2$ and $3CaO.SiO_2$ obtained by the present work shift to the left considerably. The bigger liquid region in this area might give more freedom to the steel industry for slag optimization.

For the 35 mass% Al_2O_3 section, again the results generally agree well with the lines suggested by Osborn et al. [2]. However, the present results show a slightly decreased solubility of both CaO and MgO at 1773 K. The liquidus line for the liquid-MgO equilibrium being closer to the 1723 K line suggested by Osborn et al [2] for SiO_2 contents above 10 mass%.

The liquid-CaO line at 1773 K is essentially vertical at 5.5-6 mass % silica according to the present work, about 1 mass % CaO lower compared to the work by Osborn et al [2].

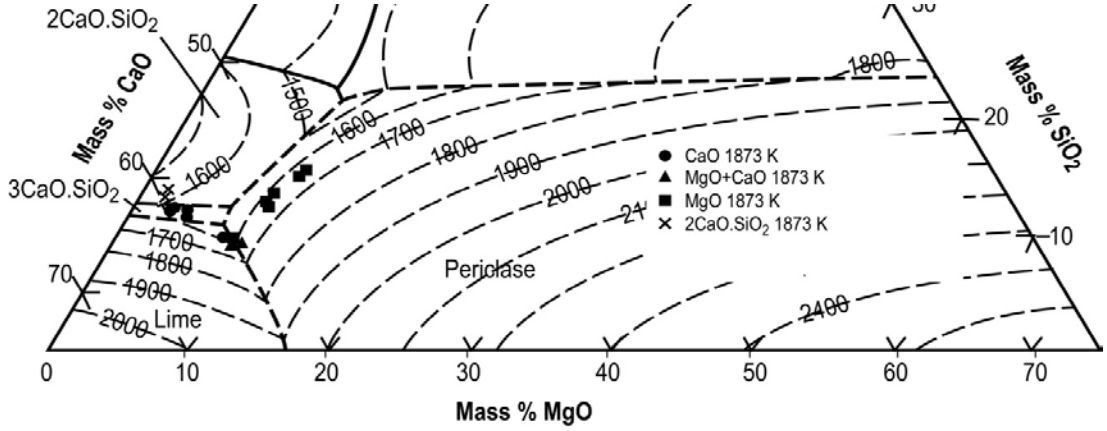

Figure 6. A comparison between the present experimental results with the phase diagram suggested by Osborn et al. [2] for 25 mass% Al_2O_3.

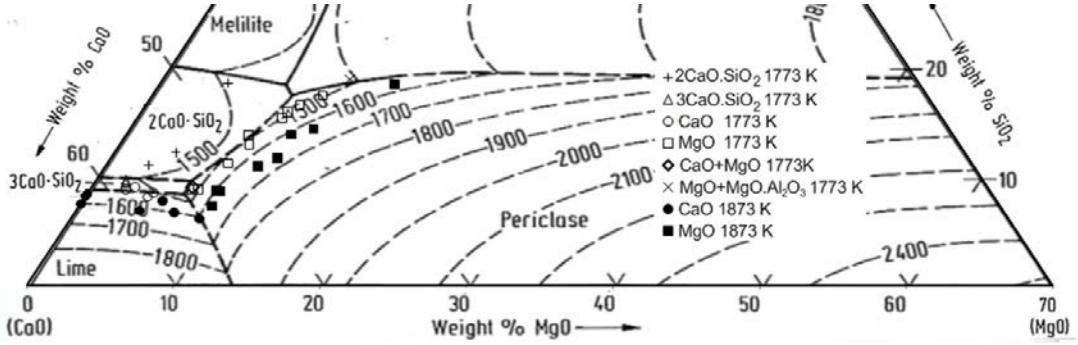

Figure 7. A comparison between the present experimental results with the phase diagram suggested by Osborn et al. [2] for 30 mass% Al_2O_3.

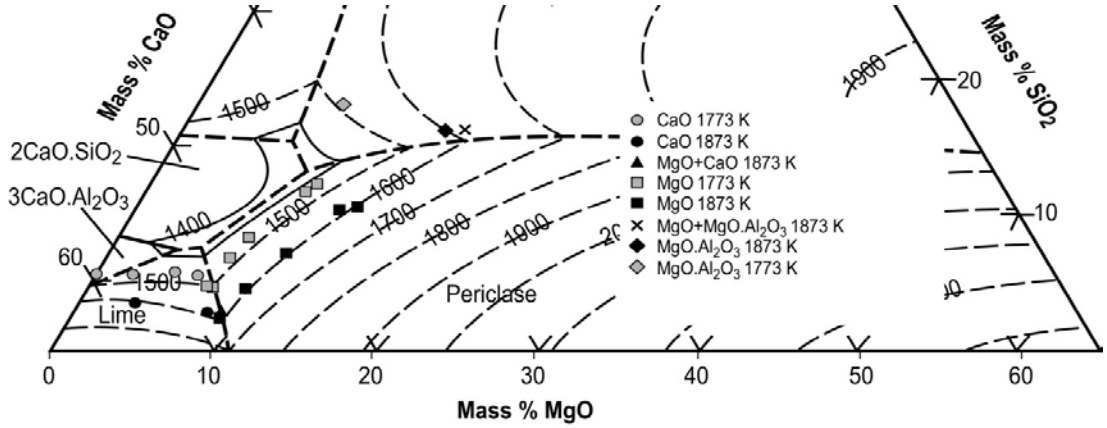

Figure 8. A comparison between the present experimental results with the phase diagram suggested by Osborn et al. [2] for 35 mass% Al_2O_3.

4.2 Estimation of the activities

The solubility of Al_2O_3, CaO, and MgO in the non-stoichiometric compounds CaO and MgO could be used to evaluate the activities of these components at the liquid-MgO and liquid-CaO equilibriums. The compositions of the compounds CaO and MgO are listed in **tables 2-4**. The 1773 K data for the 30 mass % alumina section are presented in table 2. The 1773 K data for the 25 and 35 mass percent alumina sections are presented in table 3. The 1873 K data for the 25 and 35 mass percent alumina sections are presented in table 4.

The compounds are treated as simple binaries in the evaluation of the thermodynamic activities. The partial molar Gibbs energy of the oxide components dissolved in the non-stoichiometric compound is expressed as

$$\Delta G^{M}_{MgO} = \Delta G^{XS}_{MgO\,(CaO)} + RTlnX_{MgO\,(CaO)} = RTlna_{MgO} \quad (1)$$

$$\Delta G^{M}_{CaO} = \Delta G^{XS}_{CaO\,(MgO)} + RTlnX_{CaO\,(MgO)} = RTlna_{CaO} \quad (2)$$

with the standard states being the pure solid oxides correspondingly. The notation A(B) means A dissolved in B.

The terms $\Delta G^{XS}_{MgO\,(CaO)}$ and $\Delta G^{XS}_{CaO\,(MgO)}$ are evaluated using the liquid-MgO-CaO equilibrium (sample 13, 46, 48 and 100). Since the contents of the dissolved MgO and CaO are considerably low, and in a narrow concentration region, it is assumed that the excess Gibbs energy for the component at constant temperature and pressure could be expressed with one parameter:

$$\Delta G^{XS}_{A(B)} = L_{A(B)}(1 - X_{A(B)})^2 \quad (3)$$

As the term $X_{A(B)}$ is small for all the experimental points, eq. (3) could be simplified as:

$$\Delta G^{XS}_{A(B)} = L_{A(B)} \quad (4)$$

The MgO solubility in CaO at 1873 K is evaluated from the data in table 4. The average mole fraction of MgO in solid CaO obtained in samples 46, 48 and 100 is 0.046. The activity of MgO in the MgO-phase can be taken as 0.992 (standard state: pure solid MgO) using Roults law based on the average data for samples 46, 48 and 100. Using the condition of liquid-MgO-CaO equilibrium, $L_{MgO(CaO)}$ can be evaluated using eqs.(1) and (4). The calculation leads to $L^{1873\ K}_{MgO\,(CaO)} \approx 47900$ J/mol. Using the same procedure for sample 13 in table 2, similar calculations at 1773 K gives $L^{1773\ K}_{MgO\,(CaO)} \approx 49500$ J/mol.

The CaO solubility in MgO at 1873 K can be obtained from the data for samples 46, 48 and 100 (liquid-MgO-CaO equilibrium) in table 4. The average mole fraction of CaO in solid MgO is 0.0065. The average CaO content in the CaO-phase is 0.954, which could be taken as the activity of CaO according to Roults law (standard state: pure solid CaO). Based on these data, $L^{1873\ K}_{CaO\,(MgO)}$ is calculated to be ~ 77800 J/mol using eqs.(2) and (4). Using the same procedure for sample 13 in table 2, similar calculations at 1773 K gives $L^{1773\ K}_{CaO\,(MgO)} \approx 78300$ J/mol.

For Al_2O_3 dissolved in MgO, it is evident that every unit of $AlO_{1.5}$ gives rise of 1.5 foreign particles, one Al^{3+} and half an uncharged vacancy. Therefore, for the activity estimation of Al_2O_3, the relationship derived by Hallstedt and Hillert [6] is applied;

$$a_{AlO_{1.5}} \cong f_{AlO_{1.5}} \times (X_{AlO_{1.5}})^{1.5} \quad (5)$$

The constant $f_{AlO_{1.5}}$ in eq.5 can be evaluated at 1873 K based on the liquid-MgO.Al_2O_3-MgO equilibrium in sample 98. The solubility of Al_2O_3 at the three-phase joint is 0.0088 mole fraction at 1873 K. Comparing with literature data for the binary MgO-MgO.Al_2O_3 at 1873 K, this value is in good agreement with the value reported by Mori [7], but somewhat higher than the value reported by Henriksen et al. [8]. Sample 98 has an average MgO content of X_{MgO}=0.99 in the MgO particles. This value can be taken as the activity of MgO according to Roults law. As seen in table 4, the spinel phases in sample 98 have a composition close to stochiometric MgO.Al_2O_3. Assuming that the activity MgO.Al_2O_3 is unity, the alumina activity for the MgO-MgO.Al_2O_3 equilibrium can be calculated from reaction (6).

$$MgO(s) + Al_2O_3(s) = MgO.Al_2O_3(s) \quad (6)$$

Hence,

$$a_{Al_2O_3} = \frac{1}{K_{13} a_{MgO}}$$

The standard Gibbs energy of reaction (6) can be obtained from the literature [9-10].

$\Delta G_6 = -20790 - 15.7T \ J/mol$ [9]

$\Delta G_6 = -15734 - 13.42T \ J/mol$ [10]

For the approximation of the parameter $f_{AlO_{1.5}}$, the recent data from Fujii et al. [9] is used. The handbook data from Knacke [10] is also used in the activity calculation for comparison.

The activity of Al_2O_3 at the liquid-MgO.Al_2O_3-MgO equilibrium at 1873 K is therefore calculated to be 0.0402 using the data from Fujii et al [9]. By using the relationship $(a_{AlO_{1.5}})^2 = a_{Al_2O_3}$, we get $a_{AlO_{1.5}} \approx 0.201$.

The mole fraction of $AlO_{1.5}$ in sample 98 can be approximated to be twice that of Al_2O_3 because of its low content. Inserting the activity of $AlO_{1.5}$ and $X_{AlO_{1.5}}$= 0.0176 into eq.(5) leads to $f_{AlO_{1.5}}^{1873} \approx 86$. For 1773 K, using the same procedure for sample 6 gives $f_{AlO_{1.5}}^{1773} \approx 188$.

On the basis of $L_{MgO\,(CaO)}^{1773\ K}$, $L_{MgO\,(CaO)}^{1873\ K}$, $L_{CaO\,(MgO)}^{1773\ K}$, $L_{CaO\,(MgO)}^{1873\ K}$, $f_{AlO_{1.5}}^{1773}$ and $f_{AlO_{1.5}}^{1873}$, the activities of Al_2O_3, CaO and MgO can be evaluated at 1773 and 1873 K.

The calculated activities are listed in tables 2-4.

Table 2. Composition of solid MgO and/or CaO and the estimated activities for samples in the 30 mass % alumina section at 1773 K.

Sample no.	Phases	Composition, liquid (wt%), solid (mole %)				Activity[1]			
		CaO	Al_2O_3	SiO_2	MgO	CaO	Al_2O_3		MgO
Equilibria (liquid + MgO) 1773 K									
1	Liquid	53.8	30.7	8.5	6.9	0.873	0.00013[(2)]	0.00023[(3)]	0.995
	MgO	0.431	0.076	0.005	99.488				
2	Liquid	48.4	29.6	13.5	8.4	0.436	0.00198[(2)]	0.00367[(3)]	0.996
	MgO	0.215	0.191	0.001	99.592				
3	Liquid	52.4	31.9	8.5	7.3	0.749	0.00024[(2)]	0.00044[(3)]	0.995
	MgO	0.370	0.094	0.002	99.534				
4	Liquid	49.3	32.1	10.7	8.0	0.644	0.00168[(2)]	0.00312[(3)]	0.995
	MgO	0.318	0.181	0.024	99.477				
5	Liquid	40.7	30.8	16.9	11.6	0.222	0.02078[(2)]	0.03852[(3)]	0.995
	MgO	0.109	0.418	0.006	99.467				
7	Liquid	43.8	30.8	15.4	10.0	0.412	0.00863[(2)]	0.01601[(3)]	0.995
	MgO	0.203	0.312	0.009	99.475				
8	Liquid	42.6	30.9	16.1	10.5	0.269	0.01154[(2)]	0.02139[(3)]	0.995
	MgO	0.133	0.344	0.007	99.516				
9	Liquid	47.3	31.5	12.4	8.7	0.457	0.00279[(2)]	0.00517[(3)]	0.995
	MgO	0.225	0.214	0.014	99.546				
17	Liquid	44.7	30.5	14.9	9.9	0.252	0.00695[(2)]	0.01288[(3)]	0.996
	MgO	0.125	0.290	0.005	99.580				
Equilibria (liquid + CaO) 1773 K									
12	Liquid	56.0	32.5	8.6	2.9	0.988			0.344
	CaO	98.786	0.006	0.011	1.198				
16	Liquid	57.1	32.1	8.4	2.4	0.990			0.288
	CaO	98.977	0.006	0.013	1.004				
18	Liquid	59.2	32.0	8.2	0.5	0.998			0.053
	CaO	99.805	0.002	0.009	0.183				
19	Liquid	56.0	31.4	8.2	4.4	0.980			0.579
	CaO	97.961	0.002	0.021	2.016				
21	Liquid	56.2	31.8	7.8	4.2	0.981			0.551
	CaO	98.072	0.004	0.007	1.918				
Equilibria (liquid + MgO + spinel) 1773 K									
6	Liquid	38.3	30.5	18.4	12.7	0.254	0.03715[(2)]	0.06887[(3)]	0.994
	MgO	0.125	0.508	0.009	99.358				
	Spinel	0.131	49.532	0.045	50.292				
Equilibria (liquid + MgO + CaO) 1773 K									
13	Liquid	54.6	29.6	8.8	6.9	0.965	0.00021[(2)]	0.00038[(3)]	0.994
	MgO	0.476	0.090	0.019	99.415				
	CaO	96.484	0.004	0.051	3.461				

[1.] Standard state being pure solid oxides at 1773 K [2.] Calculated using the data from [9] [3.] Calculated using the data from [10].

Table 3. Composition of solid MgO and/or CaO and the estimated activities for samples in the 25 and 35 mass % alumina section at 1773 K

Sample no.	Phases	Composition, liquid (wt%), solid (mole %)				Activity[1]			
		CaO	Al_2O_3	SiO_2	MgO	CaO	Al_2O_3		MgO
Equilibria (liquid + MgO) 1773 K									
66	Liquid	51.5	36.3	4.8	7.4	0.802	0.00043[2]	0.00080[3]	0.995
	MgO	0.396	0.115	0.001	99.488				
67	Liquid	50.8	34.5	7.1	7.6	0.688	0.00097[2]	0.00180[3]	0.995
	MgO	0.339	0.151	0.005	99.505				
68	Liquid	48.6	34.8	8.5	8.1	0.516	0.00188[2]	0.00349[3]	0.996
	MgO	0.254	0.188	0.008	99.550				
69	Liquid	43.2	35.3	11.7	9.8	0.338	0.00931[2]	0.01725[3]	0.995
	MgO	0.167	0.320	0.004	99.510				
70	Liquid	42.6	34.5	12.5	10.3	0.341	0.01456[2]	0.02700[3]	0.995
	MgO	0.168	0.372	0.006	99.454				
77	Liquid	52.9	35.0	4.9	7.2	0.880	0.00034[2]	0.00064[3]	0.993
	MgO	0.434	0.107	0.006	99.347				
Equilibria (liquid + CaO) 1773 K									
76	Liquid	58.7	35.6	5.7	0.0	1.000			0.005
	CaO	99.975	0.002	0.006	0.017				
78	Liquid	57.5	34.4	5.8	2.3	0.998			0.066
	CaO	99.755	0.008	0.009	0.229				
79	Liquid	54.7	34.6	5.9	4.8	0.979			0.602
	CaO	97.875	0.017	0.014	2.094				
80	Liquid	53.8	34.1	5.8	6.3	0.972			0.813
	CaO	97.161	0.003	0.006	2.831				
Equilibria (liquid + MgO + spinel) 1773 K									
71	Liquid	37.4	31.0	18.6	13.0	0.254	0.04201[2]	0.07788[3]	0.993
	MgO	0.125	0.529	0.010	99.335				
	Spinel	0.094	49.684	0.054	50.168				

[1.] Standard state being pure solid oxides at 1773 K. [2.] Calculated using the data from [9] [3.] Calculated using the data from [10].

Table 4. Composition of solid MgO and/or CaO and the estimated activities for samples in the 25 and 35 mass % alumina section at 1873 K

Sample no.	Phases	Composition, liquid (wt%), solid (mole %)				Activity[1]			
		CaO	Al_2O_3	SiO_2	MgO	CaO	Al_2O_3		MgO
Euilibria (liquid + MgO) 1873 K									
44	Liquid	51.5	25.6	13.5	9.4	0.516	0.00031[(2)]	0.00057[(3)]	0.994
	MgO	0.348	0.175	0.013	99.430				
45	Liquid	56.0	25.9	9.7	8.4	0.916	0.00009[(2)]	0.00017[(3)]	0.993
	MgO	0.618	0.116	0.010	99.256				
52	Liquid	48.6	26.2	14.8	10.4	0.436	0.00072[(2)]	0.00132[(3)]	0.995
	MgO	0.295	0.230	0.007	99.469				
53	Liquid	52.0	26.0	12.8	9.2	0.615	0.00020[(2)]	0.00036[(3)]	0.994
	MgO	0.416	0.150	0.007	99.427				
60	Liquid	47.5	26.9	15.0	10.5	0.368	0.00079[(2)]	0.00144[(3)]	0.995
	MgO	0.249	0.237	0.004	99.510				
61	Liquid	51.6	26.8	12.2	9.4	0.605	0.00027[(2)]	0.00049[(3)]	0.994
	MgO	0.408	0.165	0.004	99.422				
81	Liquid	52.4	36.1	2.5	9.0	0.803	0.00014[(2)]	0.00025[(3)]	0.993
	MgO	0.542	0.133	0.004	99.320				
82	Liquid	49.7	36.1	4.6	9.5	0.634	0.00029[(2)]	0.00053[(3)]	0.994
	MgO	0.428	0.170	0.003	99.399				
84	Liquid	45.6	36.7	7.1	10.6	0.412	0.00136[(2)]	0.00248[(3)]	0.994
	MgO	0.278	0.285	0.005	99.432				
87	Liquid	47.7	37.9	4.4	10.0	0.530	0.00074[(2)]	0.00135[(3)]	0.994
	MgO	0.358	0.232	0.004	99.406				
88	Liquid	50.8	37.8	2.1	9.3	0.810	0.00025[(2)]	0.00045[(3)]	0.993
	MgO	0.547	0.161	0.004	99.288				
89	Liquid	39.3	37.3	10.3	13.1	0.283	0.00755[(2)]	0.01373[(3)]	0.993
	MgO	0.191	0.503	0.004	99.302				
90	Liquid	41.2	36.3	10.3	12.3	0.340	0.00449[(2)]	0.00817[(3)]	0.993
	MgO	0.230	0.423	0.005	99.342				
Equilibria (liquid + CaO) 1873 K									
47	Liquid	56.2	26.6	9.5	7.7	0.958			0.906
	CaO	95.798	0.009	0.020	4.173				
49	Liquid	58.8	25.1	11.9	4.1	0.979			0.439
	CaO	97.949	0.002	0.027	2.021				
55	Liquid	59.0	25.8	12.2	3.0	0.985			0.318
	CaO	98.498	0.008	0.027	1.467				
58	Liquid	57.7	26.8	11.3	4.2	0.979			0.443
	CaO	97.949	0.001	0.006	2.043				
59	Liquid	56.0	26.4	10.5	7.1	0.960			0.867
	CaO	95.994	0.002	0.011	3.993				
63	Liquid	58.8	26.5	11.8	2.9	0.986			0.311
	CaO	98.553	0.003	0.011	1.433				
85	Liquid	54.3	34.5	3.0	8.3	0.962			0.829
	CaO	96.168	0.008	0.005	3.820				

[1.] Standard state being pure solid oxides at 1873 K. [2.] Calculated using the data from [9] [3.] Calculated using the data from [10].

Table 4 continued on next page.

Table 4 continued...

Sample no.	Phases	Composition, liquid (wt%), solid (mole %)				Activity[1]			
		CaO	Al_2O_3	SiO_2	MgO	CaO	Al_2O_3		MgO
Equilibria (liquid + CaO) 1873 K continued..									
86	Liquid	56.2	36.9	3.5	3.4	0.985			0.322
	CaO	98.508	0.009	0.002	1.481				
91	Liquid	54.9	38.1	1.7	5.3	0.976			0.508
	CaO	97.644	0.012	0.003	2.340				
93	Liquid	57.4	39.9	1.8	0.9	0.996			0.082
	CaO	99.612	0.006	0.006	0.376				
94	Liquid	54.3	38.4	1.0	6.3	0.970			0.640
	CaO	97.033	0.011	0.008	2.949				
95	Liquid	57.7	38.8	3.5	0.0	1.000			0.001
	CaO	99.983	0.009	0.004	0.004				
Equilibria (liquid + MgO + spinel) 1873K									
98	Liquid	31.8	33.8	16.7	17.7	0.299	0.04023[(2)]	0.07323[(3)]	0.990
	MgO	0.147	0.879	0.008	98.965				
	Spinel	0.307	49.167	0.031	50.495				
Equilibria (liquid + MgO + CaO) 1873 K									
46	Liquid	54.7	27.5	9.0	8.8	0.953	0.00008[(2)]	0.00015[(3)]	0.993
	MgO	0.628	0.111	0.006	99.255				
	CaO	95.307	0.014	0.018	4.661				
48	Liquid	55.0	27.5	9.0	8.5	0.953	0.00009[(2)]	0.00017[(3)]	0.993
	MgO	0.610	0.117	0.004	99.269				
	CaO	95.261	0.003	0.024	4.712				
100	Liquid	52.9	35.2	2.9	9.0	0.956	0.00011[(2)]	0.00021[(3)]	0.992
	MgO	0.697	0.125	0.004	99.174				
	CaO	95.641	0.004	0.003	4.353				

[1.] Standard state being pure solid oxides at 1873 K. [2.] Calculated using the data from [9] [3.] Calculated using the data from [10].

It is worthwhile mentioning that the value calculated for the activity of Al_2O_3 is strongly dependent on the choice of data for the standard Gibbs energy for formation of $MgO.Al_2O_3$. Perhaps, the most important factors affecting the accuracy of the calculated activities would be the thermodynamic data involved with the spinel phase and the assumption of stoichiometric $MgO.Al_2O_3$. While the latter is somehow justified by is composition obtained by EPMA, the effect of the presence of trace amounts of SiO_2 and CaO is not taken into consideration. The assumption of using Roults law for MgO in the MgO-phase could be somewhat ambiguous as Henrys law doesn't hold for alumina. Since it is believed the error involved in using this assumption is considerably small, Roults law is still used for simplicity. The error involved in the EPMA analysis of the liquid phase is considered very small, the uncertainty being much below one relative percent. For the solid phases, the deviation from average composition are normally a few relative percents with some exceptions around ten relative percent. Nevertheless, the present activity values would still be helpful to the researchers, as very few experimental measurements in this high basicity region are available in the literature.

5. Conclusions

In comparison with the work by Osborn at al. [2], the solubility of MgO is found higher at 1873 K for the 25 mass% Al_2O_3 section but lower at 1773 K for the 35 mass% Al_2O_3 section. The solubility of CaO is somewhat lower at 1873 K in

the 25 mass% Al_2O_3 section and at 1773 K in the 35 mass% Al_2O_3 compared to the existing phase diagram. For the 30 mass% alumina section, the solubilities of $2CaO.SiO_2$ and $3CaO.SiO_2$ at 1773 K were found to be considerably higher in comparison with the existing phase diagram. Even the solubility of MgO at 1873 K was found to be somewhat higher. However, the results generally agree very well with the results from Osborn et al.

References

[1] Slag Atlas. 2nd ed., ed. by Verein Deutscher Eisenhuttenleute, Dusseldorf: Verlag Sthaleisen GmbH; 1995, ISBN 3-514-00457-9, pp. 156-160.

[2] E. F. Osborn, R.C. DeVries, K. H. Gee and H. M. Kraner, Trans. AIME, J. Met. 6(1954), pp. 33-45.

[3] W. Gutt and A. D. Russel, J. Mat. Sci. 12(1977), pp.1869-1878.

[4] G. Cavalier and M. Sandrea-Deudon, Rev. Metall., 57(1960), pp.1143-1157.

[5] F. Dahl, J. Brandberg and Du Sichen, ISIJ Int., 46(2006), pp. 614-616.

[6] B. Hallstedt, M. Hillert, Calphad, 14(1990), pp.23-26.

[7] T. Mori, Yogyo-kyokai-shi, 90(1981), pp. 551-552.

[8] A.F. Henriksen and W.D. Kingery, Ceram. Int., 5(1979), pp 11-17.

[9] K. Fujii, T. Nagasaka and M. Hino, ISIJ Int. 40(2000), pp. 1059-1066.

[10] O. Knacke, O.Kubaschewski and K. Hesselmann. Thermochemical Properties of Inorganic Substances, 2nd ed., Springer-Verlag, Berlin, 1991, ISBN 3-540-54014-8, p. 47, 1136, 1171.